

# Hsa\_circ\_0007534 knockdown represses the development of colorectal cancer cells through regulating miR-613/SLC25A22 axis

D.-Y. DING<sup>1</sup>, D. WANG<sup>2</sup>, Z.-B. SHU<sup>1</sup>

<sup>1</sup>Department of Gastrointestinal Colorectal Surgery, China-Japan Union Hospital, Jilin University, Changchun, China

<sup>2</sup>Operation Room, China-Japan Union Hospital, Jilin University, Changchun, China

**Abstract. – OBJECTIVE:** Colorectal cancer (CRC) is a common tumor around the world. Circular RNAs (circRNAs) have been reported to be related to the development of CRC. However, the detailed mechanism is complicated. This study aimed to reveal the functional mechanism of circ\_0007534 in CRC.

**PATIENTS AND METHODS:** Quantitative real time polymerase chain reaction (qRT-PCR) and Western blot assay were performed to analyze gene expression. 3-(4,5-dimethylthiazol-2-yl)-2,5-diphenyltetrazolium bromide assay and colony formation assay were carried out to determine cell proliferation ability. Furthermore, cell migratory and invasive ability were assessed by transwell assay. Glycolytic metabolism was examined by measurements of extracellular acidification (ECAR), glucose consumption, and lactate production. Also, the interaction between circ\_0007534 or solute carrier family 25 member 22 (SLC25A22) and miR-613 was predicted and confirmed by starBase v2.0 and the Dual-Luciferase reporter assay, respectively. Mouse xenograft was performed to investigate the effect of circ\_0007534 on tumor growth *in vivo*.

**RESULTS:** Circ\_0007534 and SLC25A22 levels were up-regulated, and miR-613 level was down-regulated in CRC tissues/cells. Circ\_0007534 knockdown repressed CRC cell proliferation, colony formation, migration, invasion, and glycolysis. Interestingly, Circ\_0007534 targeted miR-613 and miR-613 targeted SLC25A22. Circ\_0007534 repressed its function by repressing miR-613 expression, and miR-613 exerted its function via inhibiting SLC25A22 expression. All together, circ\_0007534 repressed miR-613 expression and upregulate SLC25A22 level. Circ\_0007534 down-regulation repressed tumor growth *in vivo*.

**CONCLUSIONS:** We demonstrated that circ\_0007534 knockdown suppressed the growth of CRC cells by regulating miR-613/SLC25A22 axis, providing potential target for the treatment of CRC.

**Key Words:**

Circ\_0007534, miR-613, Cell development, SLC25A22, Colorectal cancer.

## Introduction

Colorectal cancer (CRC), one of the most common tumor types, is a cancer that is related to age, smoking, and diet<sup>1</sup>. CRC brings a great threaten to people's live and health. According to the statistics in 2015, there were over 376,000 new cases and approximately 191,000 deaths of CRC patients in China<sup>2</sup>. Despite some methods, including surgery and chemotherapy, were applied for the therapy of CRC, the overall survival rate was not remarkably improved<sup>3</sup>.

Circular RNAs (circRNAs) were initially considered as a type of products of splicing errors<sup>4</sup>. Nowadays, it is widely accepted that circRNAs acted as non-coding RNAs to regulate cancer cell progression, such as proliferation, migration/invasion, apoptosis, and autophagy<sup>5</sup>. Chen et al<sup>6</sup> suggested that circRNA cRAPGEF5 repressed cell proliferation and mobility by modulating miR-27a-3p expression in renal cell carcinoma. Chi et al<sup>7</sup> detected that circRNA-104075 was related to matrine-induced cell apoptosis, as well as autophagy in glioma. Furthermore, circ\_0007534, as an endogenous circRNA, was highly expressed in CRC tissues and promoted the growth of CRC cells<sup>8</sup>. However, the role of circ\_0007534 in CRC *in vivo* and the detailed mechanism remains unclear.

MicroRNAs (miRNAs), with 19-25 nucleotides in length, were identified as a family of small non-coding RNAs that modulated the level of target gene by inhibiting translation or inducing degradation of message RNA (mRNA) in human

cancers<sup>9,11</sup>. Wang et al<sup>12</sup> revealed that miR-1296-5p inhibited the proliferation, as well as the mobility of osteosarcoma cells. Zhang et al<sup>13</sup> indicated that miR-337-3p repressed cell proliferation in ovarian cancer. MiR-613 was shown to inhibit a series of cell progression in CRC, including proliferation, migration/invasion, and cycle, meaning that miR-613 played a pivotal role in CRC development<sup>14</sup>. Therefore, it is essential to explore the detailed molecular mechanism of miR-613 in CRC.

Solute carrier family 25 member 22 (SLC25A22), also known as a member of mitochondrial carrier system (MCS) family, encodes a mitochondrial glutamate carrier that transports glutamate from inner mitochondrial membrane to mitochondrial matrix<sup>15,16</sup>. SLC25A22 was related to the development of various human cancers, such as gallbladder cancer<sup>17</sup>, osteosarcoma<sup>18</sup>, and CRC<sup>19</sup>. Furthermore, SLC25A22 was reported to suppress CRC cell proliferation, mobility, and tumor growth in mice<sup>20</sup>. These data revealed that SLC25A22 exerted an important role in CRC development. Therefore, it is necessary to further explore the role of SLC25A22 in CRC.

Here, the levels of circ\_0007534, miR-613, and SLC25A22 in CRC tissues and cells were detected. Furthermore, we first explored the effect of circ\_0007534 on proliferation, migration, invasion, and glycolysis in CRC *in vitro* and elucidated a new regulatory mechanism in CRC. Besides, we proved the function of circ\_0007534 on tumor growth *in vivo*. The present study demonstrated that circ\_0007534 regulates CRC development via miR-613/SLC25A22 axis, which may provide a new light for the therapy of CRC.

## Patients and Methods

### Tissues and Cell Culture

CRC and adjacent normal tissues (N=60) were obtained from patients at China-Japan Union Hospital, Jilin University. This research was approved by the Ethics Review Committees of China-Japan Union Hospital, Jilin University. Informed consent was provided by each patient.

Normal human colon mucosal epithelial cell lines (HCT116) and two CRC cell lines (LoVo and HCT116) were provided by Shanghai Institute for Biological Sciences (Shanghai, China). All cells were kept in Roswell Park Memorial Institute-1640 (RPMI-1640) medium (Invitrogen, Carlsbad, CA, USA) containing 10% fetal bovine serum (FBS; Gibco, Rockville, MD, USA) as well as 1% penicillin/streptomycin at 37°C with 5% CO<sub>2</sub>.

### RNA Extraction and Quantitative Real Time-Polymerase Chain Reaction (qRT-PCR)

Total RNA was obtained using TRIzol reagents (Invitrogen, Carlsbad, CA, USA) according to the user's manual. Next, the first strand cDNA synthesis kit (TaKaRa, Komatsu, Japan) was employed to generate complementary DNA (cDNA), and then qRT-PCR was carried out with the use of the SYBR Green dye (TaKaRa, Komatsu, Japan). The level of gene was normalized to β-actin or glyceraldehyde 3-phosphate dehydrogenase (GAPDH) using the 2<sup>-ΔΔCt</sup> method. The primer sequences were: circ\_0007534, forward (F) 5'-GTGACGGAAATCAATTGCC-3' and reverse (R) 5'-ATGCCCTGCTGGCC-3'; miR-613, F 5'-CAAAATCCTTCTTTC-3' and R 5'-GAACAIGTCTCTATCTC-3'; SLC25A22, F 5'-CAACGAGGCTCTACTCTG-3' and R 5'-GGTAGTAGACCAAGTGCGAT-3'; U6, F 5'-TGCGGGTGCTCGCTTCGGCAGC-3' and R 5'-CCAGTCAGGTCGAGGT-3'; GAPDH, F 5'-GCACGTCAAGCTGAGAAC-3' and R 5'-GTGATACGCCAGTGGA-3', 18S rRNA, F 5'-CTGGTTGATCCTGCCAGT-3' and R 5'-GGCACCAGACTTGCCCTC-3'.

### Cytoplasmic and Nuclear Fractionation Location

The PARIS Kit (Life Technologies, Carlsbad, CA, USA) was employed for cytoplasmic fractionation in line with the recommended instruction. Briefly, the cells were incubated with lysis buffer for 10 min, and then, centrifuged at 4°C. Then, the supernatant and pellets were used to extract cytoplasmic RNA and nuclear RNA, respectively. Finally, the levels of RNAs in nuclear and cytoplasm were analyzed by qRT-PCR.

### RNase R Treatment

For the measurement of circ\_0007534 stabilization, the total RNA (5 μg) was incubated with RNase R (3 U/μg; Epicentre Biotechnologies, Madison, WI, USA) for 15 min at 37°C for 2 times. Subsequently, qRT-PCR was performed to analyze the levels of circ\_0007534 and linear mRNA (GAPDH).

### Cell Transfection

The small interfering RNA against circ\_0007534 (si-circ\_0007534; GenePharma Co., Ltd., Shanghai, China) and miR-613 inhibitor (anti-miR-613; GenePharma Co., Ltd., Shanghai, China) were applied to deplete circ\_0007534 and miR-613, respectively. For overexpression of SLC25A22, its

sequence was inserted into the pcDNA3.1 vector (GenePharma Co., Ltd., Shanghai, China). The cells were transfected using Lipofectamine 3000 (Invitrogen, Carlsbad, CA, USA).

#### **Cell Proliferation Assay**

Cell proliferation ability was assessed by 3-(4,5-dimethylthiazol-2-yl)-2, 5-diphenyltetrazolium bromide (MTT) kit (Promega, Madison, WI, USA) in line with the recommended protocol. In brief, the cells were transfected, and then, cultured for 0 h, 12 h, 24 h, or 48 h. Then, the cells were incubated with MTT solution, and then dissolved using dimethyl sulfoxide (DMSO). Finally, optical density was examined by ELx800 absorbance reader (BioTek Instruments, Winooski, VT, USA) at 490 nm.

#### **Colony Formation Assay**

Briefly, the cells were transfected, and kept in 6-well plates for 14 d. Then, the cells were washed using PBS, fixed by paraformaldehyde, and then, stained with 0.5% crystal violet. Finally, a microscope (Olympus, Tokyo, Japan) was used to take a picture, and then, the number of the clone was counted.

#### **Cell Migration and Invasion Assay**

In briefly, transfected cells in 100  $\mu$ L serum-free medium were introduced into the top of transwell chamber (BD Biosciences, Franklin Lakes, NJ, USA), and the bottom of the chamber was introduced with 500  $\mu$ L medium containing 10% FBS. After 24 h, migratory cells on the bottom were counted by a microscope (Olympus, Tokyo, Japan). For cell invasion, Matrigel (BD Biosciences, Franklin Lakes, NJ, USA) was coated on the insert, and the steps were in agreement with that in cell migratory assay.

#### **Western Blot Assay**

Total proteins in CRC tissues and cells were isolated using lysis buffer (Beyotime, Shanghai, China). The Western blot assay was performed in line with the previous steps<sup>21</sup>. Briefly, the proteins were separated, transferred onto polyvinylidene difluoride membranes (PVDF; Millipore, Billerica, MA, USA), and blocked by 5% bovine-fat milk. After that, the membranes were probed with the primary antibodies against matrix metalloproteinase 2 (MMP-2), MMP-9, hexokinase 2 (HK2), Glucose transporter 1 (GLUT1), lactate dehydrogenase A (LDHA), SLC25A22, and GAPDH (1:1,000; Abcam, Cam-

bridge, MA, USA). After incubation by the corresponding secondary antibodies (1:2,000; Abcam, Cambridge, MA, USA), the protein bands were measured using enhanced chemiluminescent (ECL) agents (BD Biosciences, Franklin Lakes, NJ, USA).

#### **The Measurement of ECAR**

Firstly, the cells were transfected, and kept in 6-well plates. Next, ECAR was determined using the Seahorse XF analyzer (Agilent Technologies, Santa Clara, CA, USA) as previously described<sup>22</sup>.

#### **The Measurement of Glucose Consumption and Lactate Production**

Glucose consumption and lactate production were analyzed by Glucose Assay kit (Sigma-Aldrich, St. Louis, MO, USA) and Lactate Assay kit (Sigma-Aldrich, St. Louis, MO, USA), respectively. The experiments were carried out as previously described<sup>23</sup>.

#### **The Dual-Luciferase Reporter Assay**

Wild-type or mutant-type of circ\_0007534 or SLC25A22 3'-untranslated region (UTR) was cloned into the pGL3 vector (Promega, Madison, WI, USA). Then, the cells were transfected with the reporter and miR-613 or miR-NC. After 48 h, luciferase density was examined using the Dual-Luciferase Reporter Assay System (Promega, Madison, WI, USA).

#### **Mouse Xenografts**

4-week-old BALB/c nude mice were used in this research. This assay was performed in line with the guidance of the National Animal Care and Ethics Institution. Briefly, LoVo cells transfected with small hairpin RNA against circ\_0007534 (sh-circ\_0007534) or sh-NC (GenePharma Co., Ltd) were subcutaneously injected into the mice. Then, tumor volume (length  $\times$  width<sup>2</sup>/2) was calculated every 7 d. After 35 d, the tumor was removed, and tumor weight was analyzed. This study was approved by the Animal Research Committee of China-Japan Union Hospital, Jilin University.

#### **Statistical Analysis**

The results were obtained from at least three independent experiments, analyzed by Student's *t*-test or Analysis of Variance (ANOVA) with Tukey's honestly significant difference (HSD) post-hoc test, and expressed as the means  $\pm$  standard deviation (SD). The relationship between

the levels of the two genes was explored through the analysis of Pearson's correlation coefficient.  $p < 0.05$  was considered significant.

## Results

### *Circ\_0007534 Level was Upregulated in CRC Tissues and Cells*

We first analyzed the level of circ\_0007534 in CRC tissues and adjacent normal tissues from CRC patients (Table I) and found that circ\_0007534 level was significantly upregulated in CRC tissues (Figure 1A). Then, circ\_0007534 level in CRC cells was investigated. As shown in Figure 1B, its level was higher in CRC cells than that in normal cells. Next, we analyzed the distribution of circ\_0007534 in LoVo and SW620 cells. The results suggested that circ\_0007534 was mainly located in cytoplasm (Figure 1C and D). On the other hand, RNase R was used to detect the stabilization of circ\_0007534. Compared with linear RNA, circ\_0007534 was resistant against RNase R (Figure 1E and F). Besides, we found that circ\_0007534 level in CRC patients with high survival rate was lower than that in CRC patients with low survival rate (Figure 1G). These data indicated that circ\_0007534 expression was positively correlated with CRC development.

### *Circ\_0007534 Knockdown Inhibited Cell Proliferation, Colony Formation, Migration, Invasion, and Glycolysis in CRC Cells*

To investigate the effect of circ\_0007534 on the growth of CRC cells, LoVo and SW620 cells were transfected with si-circ\_0007534 knockdown

circ\_0007534. Si-NC was used as negative control. Knockdown efficiency was confirmed by qRT-PCR (Figure 2A and B). Next, cell proliferation ability was determined by MTT assay. As demonstrated in Figure 2C and D, circ\_0007534 knockdown dramatically inhibited cell proliferation. Moreover, colony formation assay suggested that the number of colonies was significantly decreased due to circ\_0007534 knockdown (Figure 2E). Subsequently, transwell assay was used to assess cell migration. The results revealed that circ\_0007534 knockdown remarkably suppressed cell migration and invasion (Figure 2F and G; 100% similarity). Similarly, the levels of two proteins (MMP2 and MMP9) related to cell migration and invasion were downregulated by circ\_0007534 knockdown (Figure 2H and I).

On the other hand, we analyzed whether circ\_0007534 affected glycolytic metabolism by measuring extracellular acidification rate (ECAR). The results indicated that ECAR was reduced by circ\_0007534 knockdown in LoVo and SW620 cells (Figure 2J and K). Furthermore, our results showed that circ\_0007534 knockdown decreased glucose consumption and lactate production (Figure 2L and M). In addition, circ\_0007534 knockdown significantly downregulated the levels of glycolysis-associated GLUT1, HK2, and PFKFB3 (Figure 2N and O). Therefore, circ\_0007534 knockdown inhibited the growth of CRC cells.

### *Circ\_0007534 Targeted miR-613*

Through bioinformatics tool starBase v2.0, we found that miR-613 was a potential target of circ\_0007534 (Figure 3A). Then, the Dual-Luciferase reporter assay was performed to verify

**Table I.** Correlation between circ\_0007534 level and pathological indexes of colorectal cancer patients (n=60).

Parameter	Case	circ_0007534 expression		p-value <sup>a</sup>
		Low (n=27)	High (n=33)	
Age (years)	≤50	16	29	0.4846
	>50	11	14	
Gender	Male	10	14	0.6717
	Female	17	19	
Tumor size	≤3 cm	23	16	0.0030*
	>3 cm	4	17	
Lymph node metastasis	Absent	19	10	0.0020*
	Present	8	23	

\* $p < 0.05$ ; <sup>a</sup>Chi-square test.

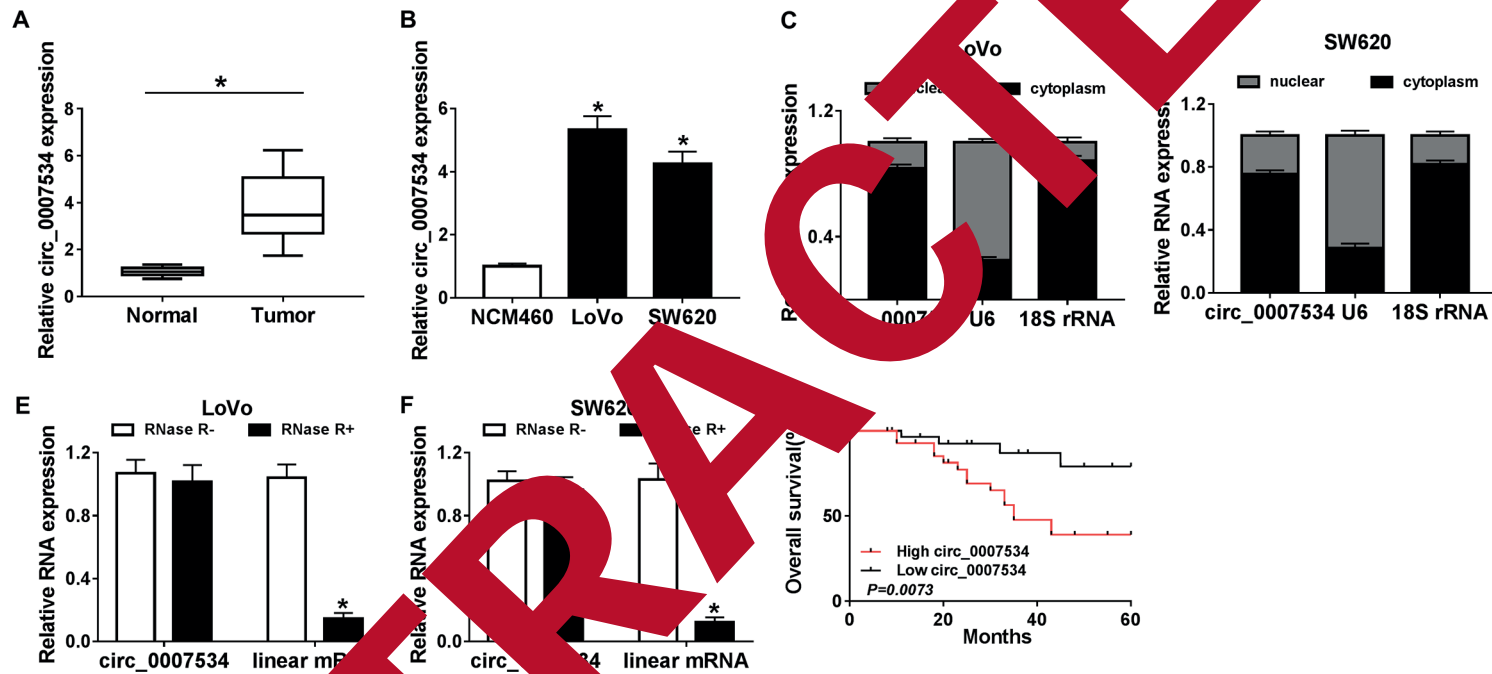


**Figure 1.** Circ\_0007534 was up-regulated in CRC tissues/cells and related to overall survival rate. **A**, Circ\_0007534 level was detected by qRT-PCR in CRC tissues and adjacent normal tissues. **B**, Circ\_0007534 level was determined in CRC cells and normal cells. **C**, and **D**, The levels of circ\_0007534, U6, and 18S rRNA were measured in nuclear and cytoplasmic fractions of LoVo and SW620 cells. **E**, and **F**, The levels of circ\_0007534 and linear mRNA were examined after the treatment of RNase R. **G**, The relationship between circ\_0007534 and overall survival rate of CRC patients was analyzed. \* $p < 0.05$ .

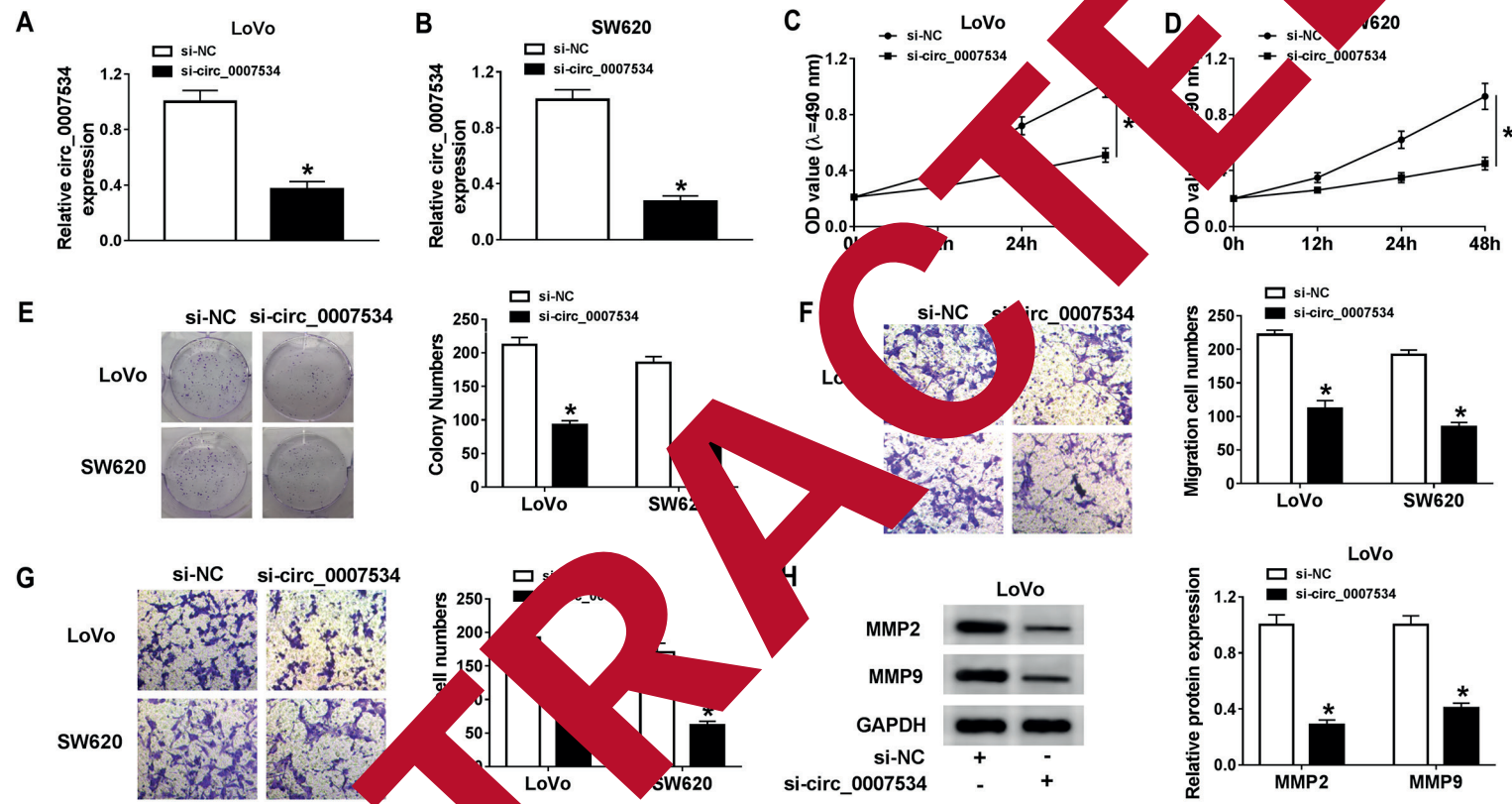


**Figure 2.** Circ\_0007534 was an oncogene in CRC. **A**, and **B**, The expression of circ\_0007534 was detected in LoVo and SW620 cells transfected with si-NC or si-circ\_0007534. **C**, and **D**, CCK-8 assay was performed to assess cell proliferation ability. **E**, Colony formation assay was carried out. **F**, and **G**, Cell migratory and invasive abilities were determined using transwell assay (magnification 100X). **H**, and **I**, The levels of MMP2 and MMP9 were examined by Western blot assay. **J**, and **K**, XF 96 was used to determine the levels of LAR. **L**, and **M**, Glucose consumption and lactate production were investigated by related kits. **N**, and **O**, Western blot assay was performed to detect the levels of HK2, GLUT1, and LDHA. \* $p < 0.05$ .

Figure continued

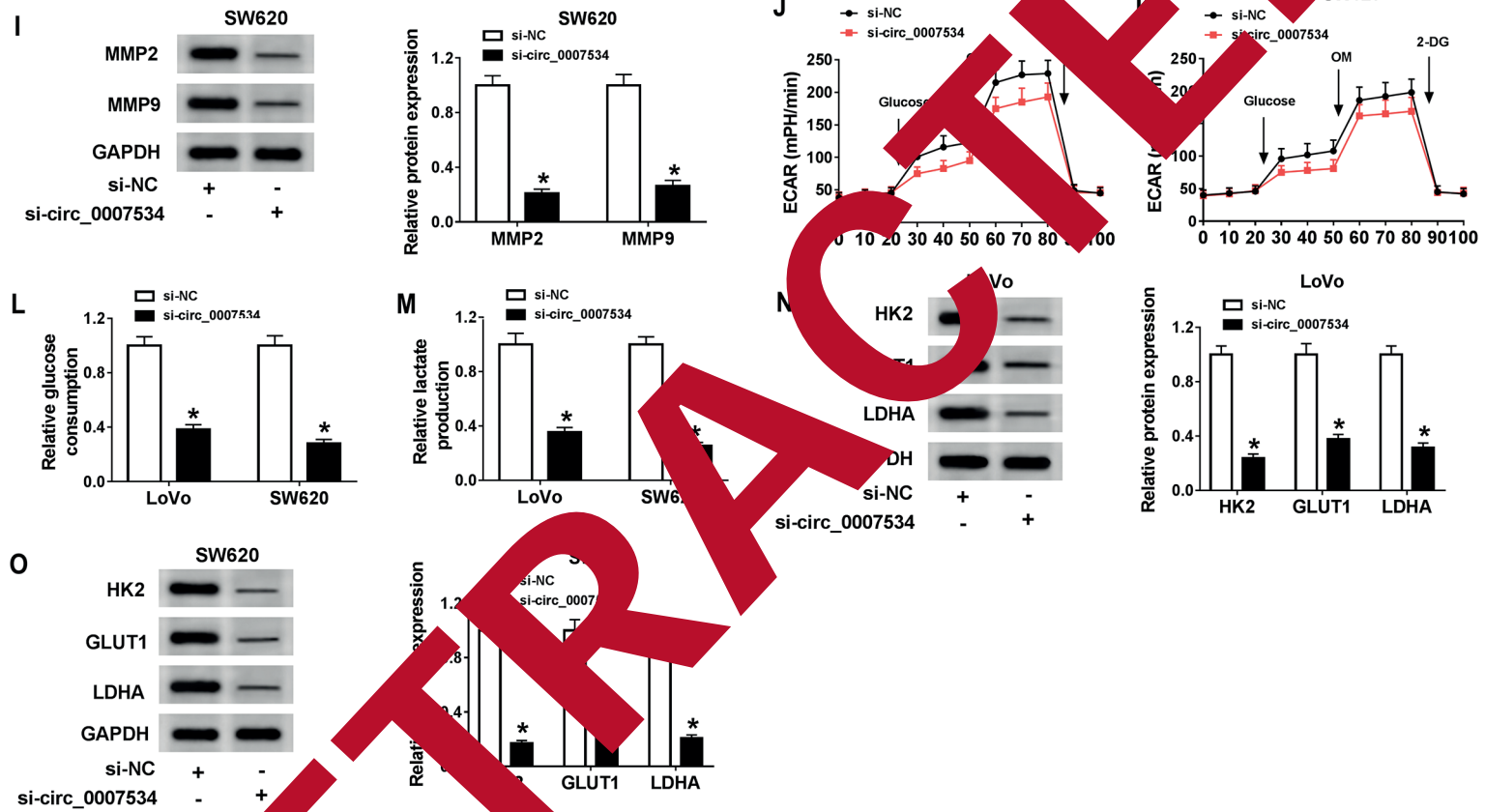


**Figure 2 (Continued)** **J** and **K**, XF 96 was used to determine ECAR. **L**, and **M**, Glucose consumption and lactate production were investigated by related kits. **N**, and **O**, Western blot assay was performed to detect the levels of HK2, GLUT1, and LDHA. \* $p < 0.05$ .

fy this interaction by transfecting circ\_0007534 WT or circ\_0007534 MUT and miR-613 or miR-NC into LoVo and SW620 cells. As shown in Figure 3B and C, miR-613 remarkably reduced the Luciferase activity of circ\_0007534 WT but didn't affect the Luciferase activity of circ\_0007534 MUT. This result revealed that miR-613 interacted with circ\_0007534. Next, the effect of circ\_0007534 on miR-613 expression was investigated. The results demonstrated that circ\_0007534 knockdown dramatically increased miR-613 expression in LoVo and SW620 cells (Figure 3D). In addition, we determined the level of miR-613 in CRC tissues and cells, finding that miR-613 level was lower in CRC tissues/cells than that in normal tissues/cells (Figure 3E and F). Besides, the relationship between miR-613 expression and circ\_0007534 expression was analyzed. As expected, miR-613 expression was negatively correlated with circ\_0007534 expression (Figure 3G). These data confirmed that circ\_0007534 targeted miR-613 and repressed its expression.

#### **MiR-613 Depletion Weakened the Effect of Circ\_0007534 Knockdown on the Development of CRC Cells**

To investigate whether circ\_0007534 exerted its function *via* modulating miR-613 expression, LoVo, and SW620 cells were transfected with si-NC, si-circ\_0007534, si-circ\_0007534 + anti-miR-613, or si-circ\_0007534 + anti-miR-613, respectively. QRT-PCR showed that miR-613 expression was upregulated by circ\_0007534 knockdown and then, downregulated due to the transfection with anti-miR-613 (Figure 4A and B). MTT assay suggested that cell proliferation was greatly inhibited by circ\_0007534 knockdown, which was almost completely reversed by miR-613 depletion (Figure 4C and D). Moreover, miR-613 depletion weakened the inhibitory effect of circ\_0007534 knockdown on colony formation (Figure 4E). Next, transwell assay was employed to assess cell viability. As demonstrated in Figure 4F and G, circ\_0007534 knockdown significantly suppressed cell migration and invasion, whereas these functions were impaired by miR-613 depletion in LoVo and SW620 cells. Similarly, the positive effect of miR-613 depletion on circ\_0007534 knockdown-mediated downregulated levels of MMP2 and MMP9 was observed in CRC cells (Figure 4H and I).

On the other hand, the effect of miR-613 on circ\_0007534-regulated glycolytic metabolism was explored *via* determining ECAR. As shown

in Figure 4J and K, ECAR was downregulated by circ\_0007534 knockdown, and then partly rescued due to miR-613 depletion. Moreover, the negative effect of circ\_0007534 knockdown on glucose consumption and lactate production was reversed by miR-613 depletion (Figure 4L and M). Besides, we found that circ\_0007534 knockdown-mediated downregulated levels of GLUT1, HK2, and LDH were upregulated by miR-613 depletion (Figure 4N and O). Therefore, circ\_0007534 inhibited miR-613 expression to regulate CRC cell development.

#### **MiR-613 was a Strong Regulator of SLC25A22**

Next, we used bioinformatics tool StarBase v2.0 to predict potential targets of miR-613. The results suggested that SLC25A22 possessed a complementary sequence with miR-613 (Figure 5A). Then, the Dual-Luciferase reporter assay was performed to confirm the interaction between miR-613 and SLC25A22. As shown in Figure 5B, the Luciferase activity of SLC25A22 3'-UTR-WT but not SLC25A22 3'-UTR-MUT, was remarkably diminished by miR-613 overexpression, meaning that miR-613 bound to SLC25A22. Subsequently, the effect of miR-613 on SLC25A22 expression was explored. The results indicated that miR-613 depletion significantly increased the expression of SLC25A22 in LoVo and SW620 cells (Figure 5C and D). In addition, we analyzed the level of SLC25A22 in CRC tissues and cells and found that SLC25A22 level was higher in CRC tissues/cells than that in normal tissues/cells (Figure 5F-I). Besides, our results demonstrated that SLC25A22 expression was negatively correlated with miR-613 expression in CRC tissues (Figure 5J). These data showed that miR-613 targeted SLC25A22 and repressed SLC25A22 expression.

#### **SLC25A22 Overexpression Reversed the Effect of MiR-613 Upregulation on the Development of CRC Cells**

To analyze whether miR-613 exerted function *via* regulating SLC25A22 expression, LoVo and SW620 cells were transfected with miR-NC, miR-613, miR-613 + Vector, or miR-613 + SLC25A22, respectively. QRT-PCR revealed that SLC25A22 expression was downregulated by miR-613 overexpression and upregulated by the transfection with SLC25A22 (Figure 6A-C). Then, MTT assay was carried out to determine cell proliferation ability. As shown in Figure 6D and E, miR-613 overexpression greatly suppressed cell proliferation, whereas this action was weakened due to SLC25A22 up-



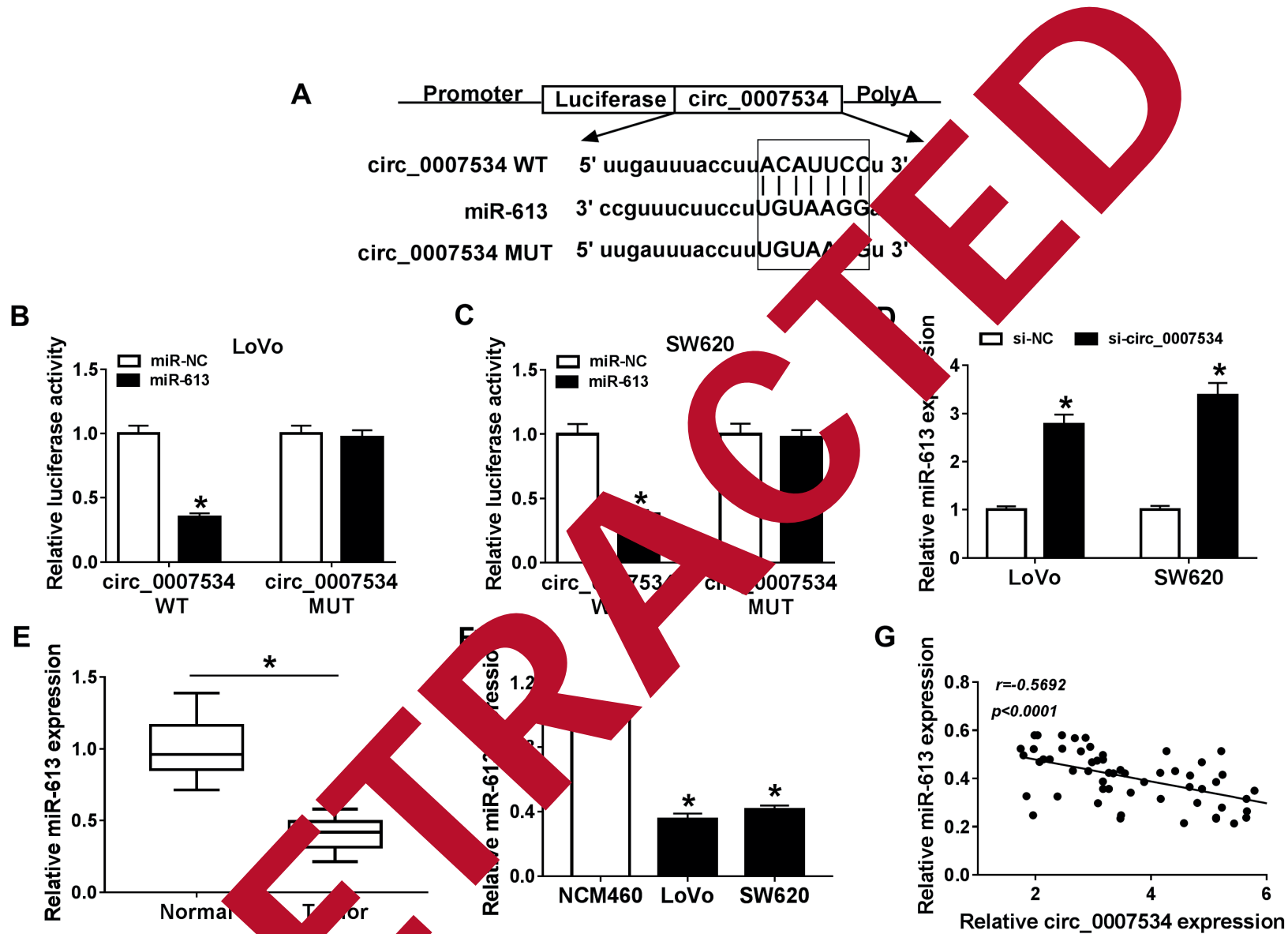


**Figure 3.** Circ\_0007534 sponge miR-613 in CRC. **A**, The interaction between circ\_0007534 and miR-613 was predicted by starBase v2.0. **B**, and **C**, The Luciferase activity of LoVo and SW620 cells transfected with circ\_0007534 WT or circ\_0007534 MUT and miR-613 or miR-NC was measured. **D**, MiR-613 expression was determined in LoVo and SW620 cells transfected with si-NC or si-circ\_0007534. **E**, and **F**, The level of miR-613 was detected in CRC and normal tissues (**E**), as well as CRC and normal cells (**F**). **G**, The relationship between circ\_0007534 expression and miR-613 expression was analyzed. \* $p < 0.05$ .

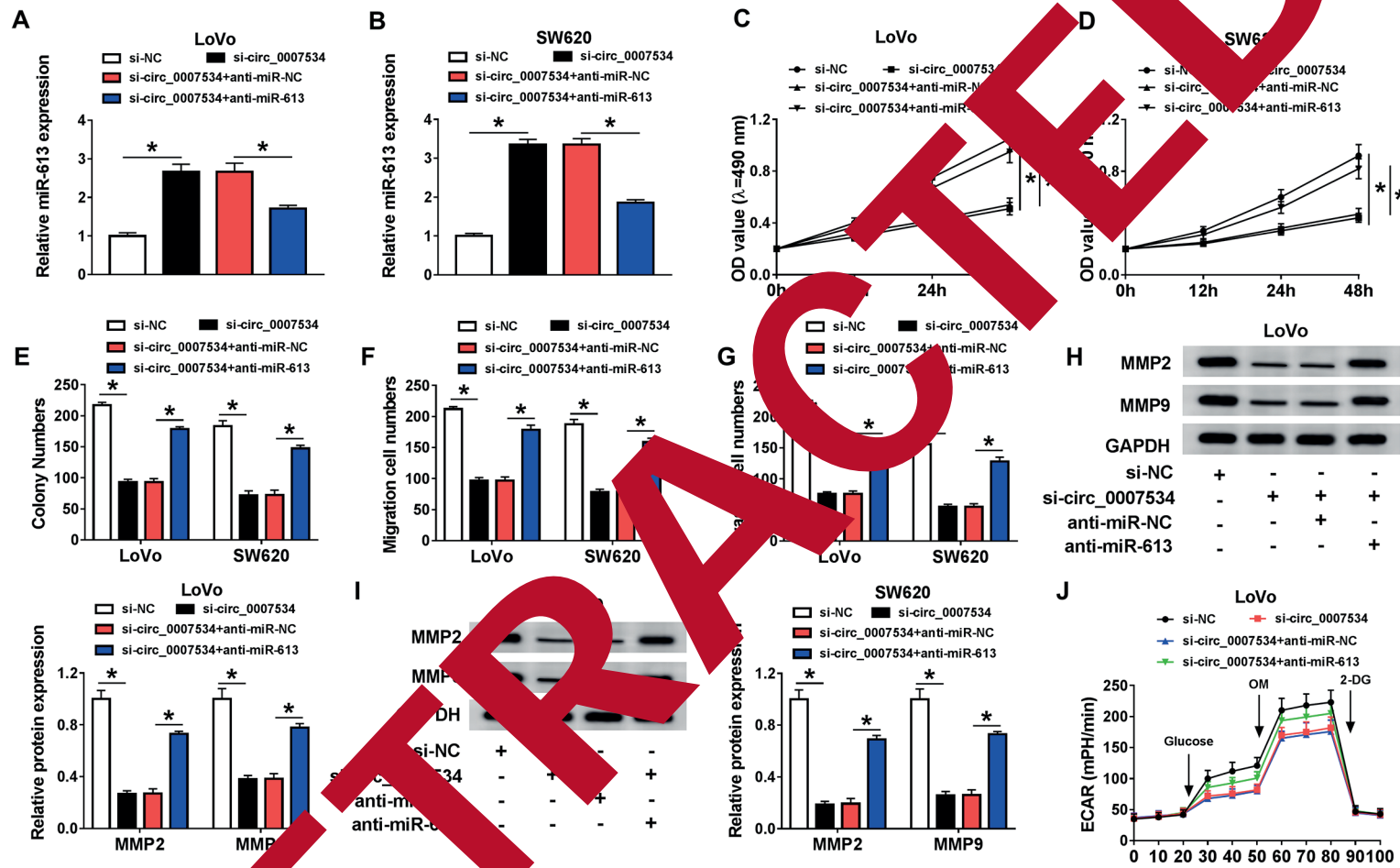


**Figure 4.** Circ\_0007534 promoted CRC cell progression by inhibiting miR-613 expression. **A**, and **B**, The expression of miR-613 was detected in LoVo and SW620 cells transfected with si-NC, si-circ\_0007534, si-circ\_0007534 + anti-miR-NC, or si-circ\_0007534 + anti-miR-613, respectively. **C**, and **D**, Cell proliferation ability was examined by MTT assay. **E**, Colony formation assay was performed. **F**, and **G**, Transwell assay was carried out to measure cell migratory and invasive abilities. **H**, and **I**, The levels of MMP2 and MMP9 were determined by Western blot assay. **J**, and **K**, XF 96 was employed to determine ECAR. **L**, and **M**, Glucose consumption and lactate production were measured by related kits. **N**, and **O**, Western blot assay was used to measure the levels of HK2, GLUT1, and LDHA. \* $p < 0.05$ .

Figure continued

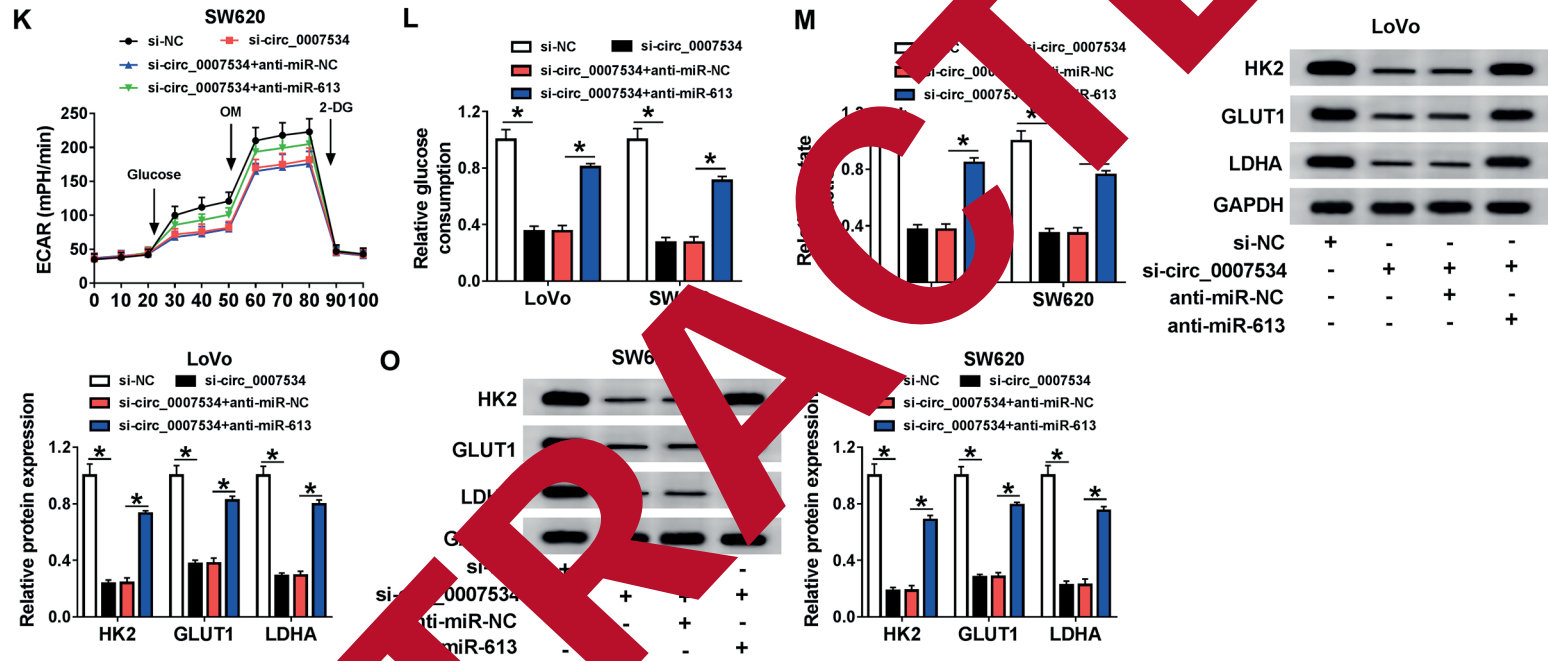


**Figure 4 (continued).** J, and K, XF 96 was employed to determine ECAR. L, and M, Glucose consumption and lactate production were analyzed by related kits. N, and O, Western blot assays were used to measure the levels of HK2, GLUT1, and LDHA. \* $p < 0.05$ .

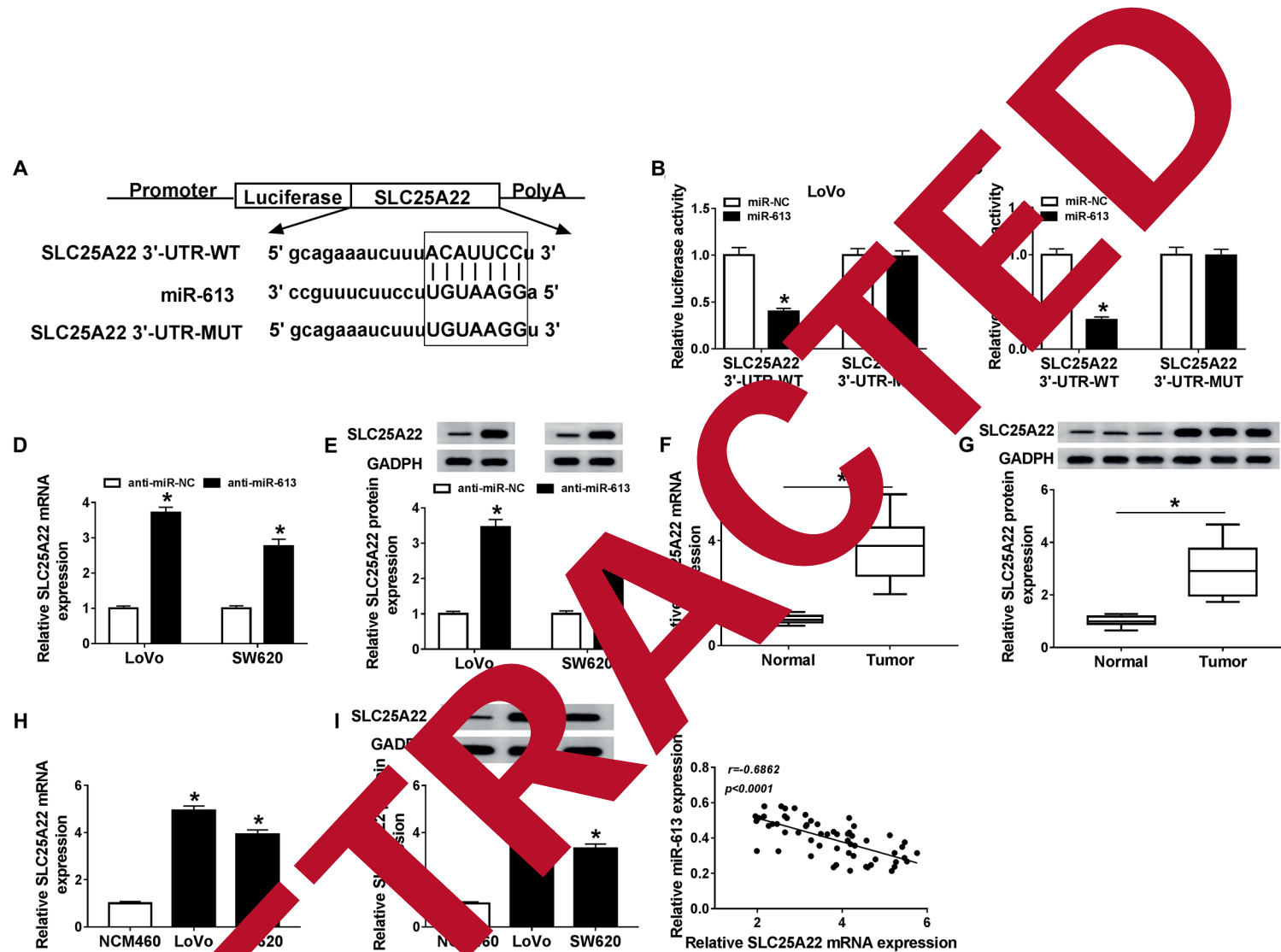


**Figure 5.** MiR-613 was a negative regulator of SLC25A22. **A**, The interaction between miR-613 and SLC25A22 was predicted by starBase v2.0. **B**, and **C**, The Luciferase activity was determined in LoVo and SW620 cells transfected with SLC25A22 3'-UTR-WT or SLC25A22 3'-UTR-MUT and miR-613 or miR-NC. **D**, and **E**, SLC25A22 expression was detected in LoVo and SW620 cells transfected with anti-miR-NC or anti-miR-613. **F-I**, The level of SLC25A22 was examined in CRC and normal tissues (**F** and **G**), as well as LoVo and normal cells (**H** and **I**). **J**, The relationship between SLC25A22 expression and miR-613 expression was investigated. \* $p < 0.05$ .

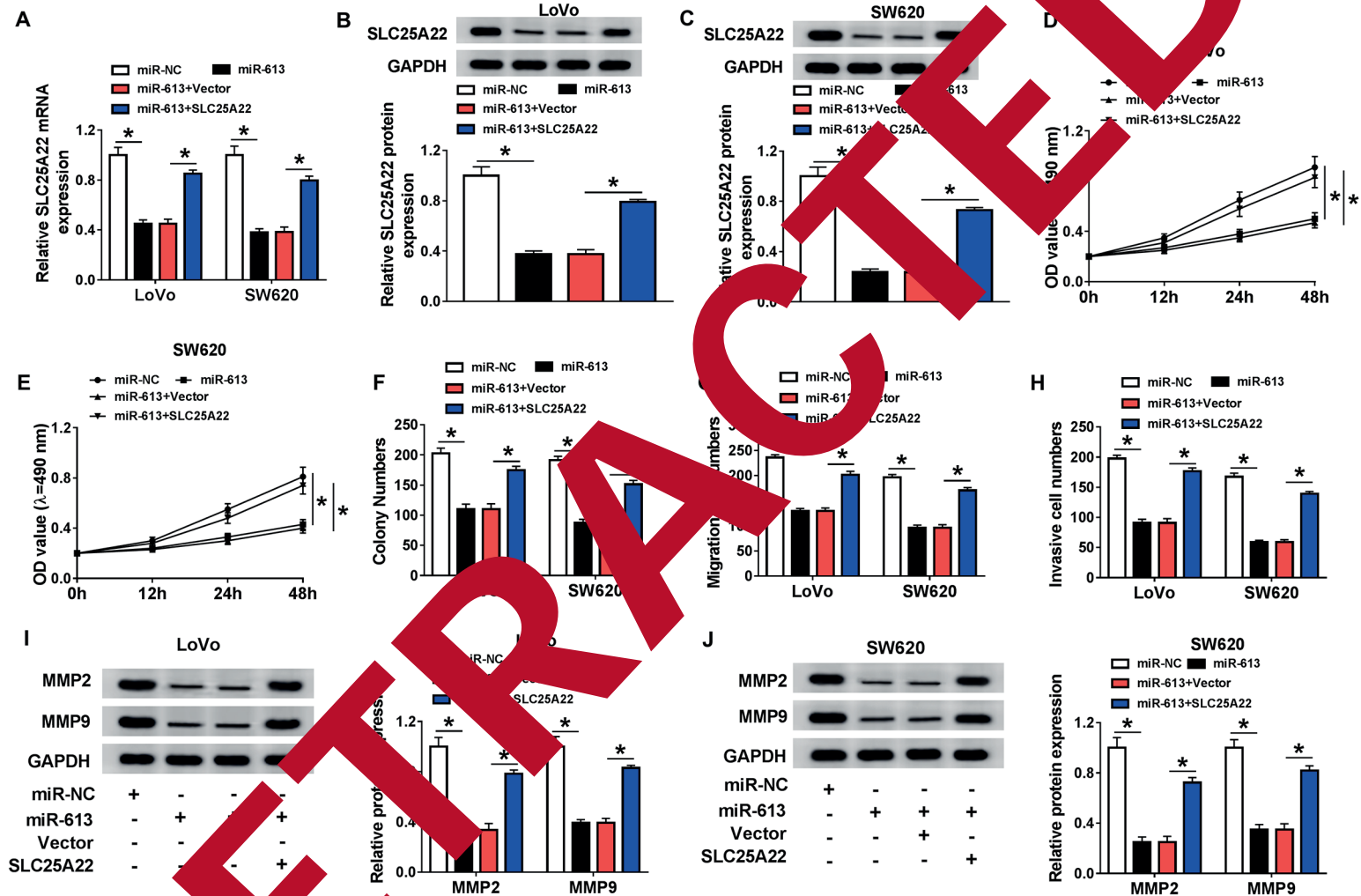


**Figure 6.** MiR-613 modulates LoVo cell progression via repressing SLC25A22 expression. **A-C**, The expression of SLC25A22 was detected by qRT-PCR and western blot analysis. LoVo and SW620 cells were transfected with miR-NC, miR-613, miR-613 + Vector, or miR-613 + SLC25A22, respectively. **D**, and **E**, MTT assay was carried out to measure cell proliferation ability. **F**, Colony formation assay was performed. **G**, and **H**, Cell migratory and invasive abilities were examined by transwell assay. **I**, and **J**, the levels of MMP2 and MMP9 were detected by Western blot assay.

Figure continued

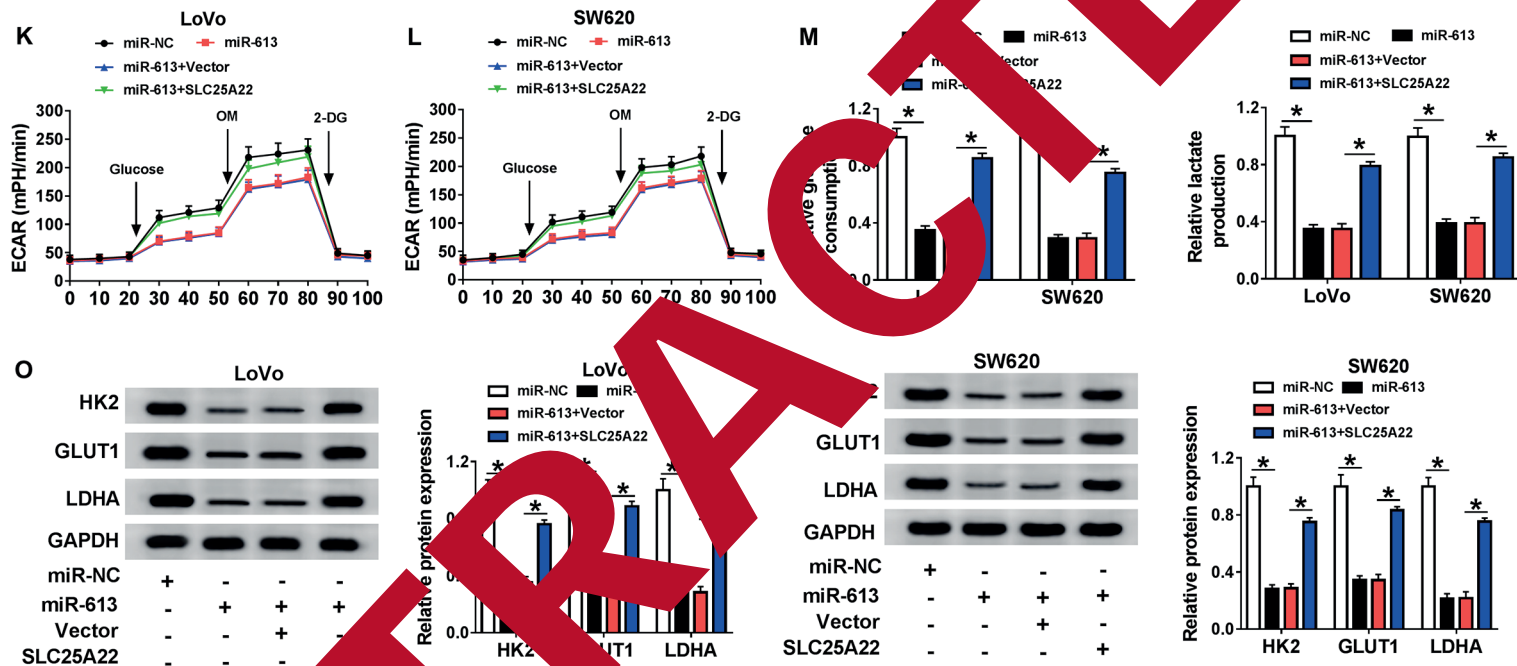


**Figure 6. (Continued).** K and L, XF 96 was employed to analyze ECAR. M, and N, Glucose consumption and lactate production were explored by related kits. O, and P, The levels of HK2, GLUT1, and LDHA were determined by Western blot assay. \* $p < 0.05$ .

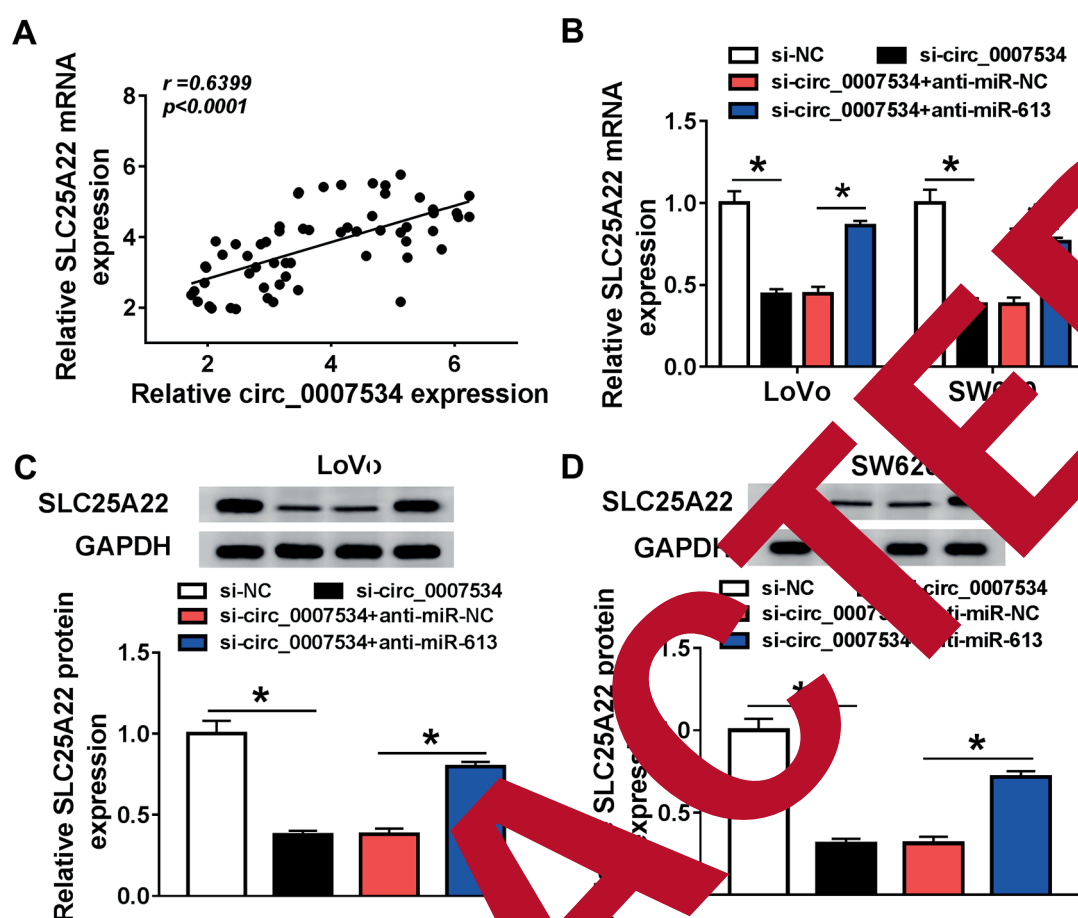


**Figure 7.** The linear relationship between circ\_0007534, miR-613, and SLC25A22 was investigated. **A**, The relationship between SLC25A22 expression and circ\_0007534 expression was investigated. **B-D**, The expression of SLC25A22 was detected in LoVo and SW620 cells treated with si-NC, si-circ\_0007534, si-circ\_0007534 + anti-miR-NC, or si-circ\_0007534 + anti-miR-613, respectively. \* $p < 0.05$ .

regulation. For tumor colony formation assay showed that SLC25A22 upregulation reversed the effect of miR-613 overexpression on colony formation (Figure 6F). Next, cell motility was assessed by Transwell assay. The results demonstrated that cell migration and invasion were dramatically suppressed by miR-613 overexpression, and then partially rescued by SLC25A22 upregulation (Figure 6G and H). Similarly, the positive effect of SLC25A22 upregulation on miR-613 overexpression-downregulated levels of MMP2 and MMP9 was observed in CRC cells (Figure 6I and J).

We analyzed glycolytic metabolism in this study and found that miR-613 overexpression decreased ECAR, and this action was impaired due to SLC25A22 upregulation in LoVo and SW620 cells (Figure 6K and L). Moreover, SLC25A22 upregulation reversed the effect of miR-613 over-

expression on glucose consumption and lactate production (Figure 6M and N). In addition, we found that miR-613 overexpression-mediated downregulated levels of GLUT1, HK2, and LDH were upregulated by SLC25A22 upregulation (Figure 6O and P). These data indicated that miR-613 regulated CRC cell development by inhibiting SLC25A22 expression.

#### **Circ\_0007534 Upregulated SLC25A22 Level Through Inhibiting MiR-613 Expression**

Next, the relationship between the levels of SLC25A22 and circ\_0007534 was investigated. As expected, SLC25A22 level was positively correlated with circ\_0007534 level in CRC tissues (Figure 7A). Therefore, we speculated that circ\_0007534 promoted SLC25A22 expression

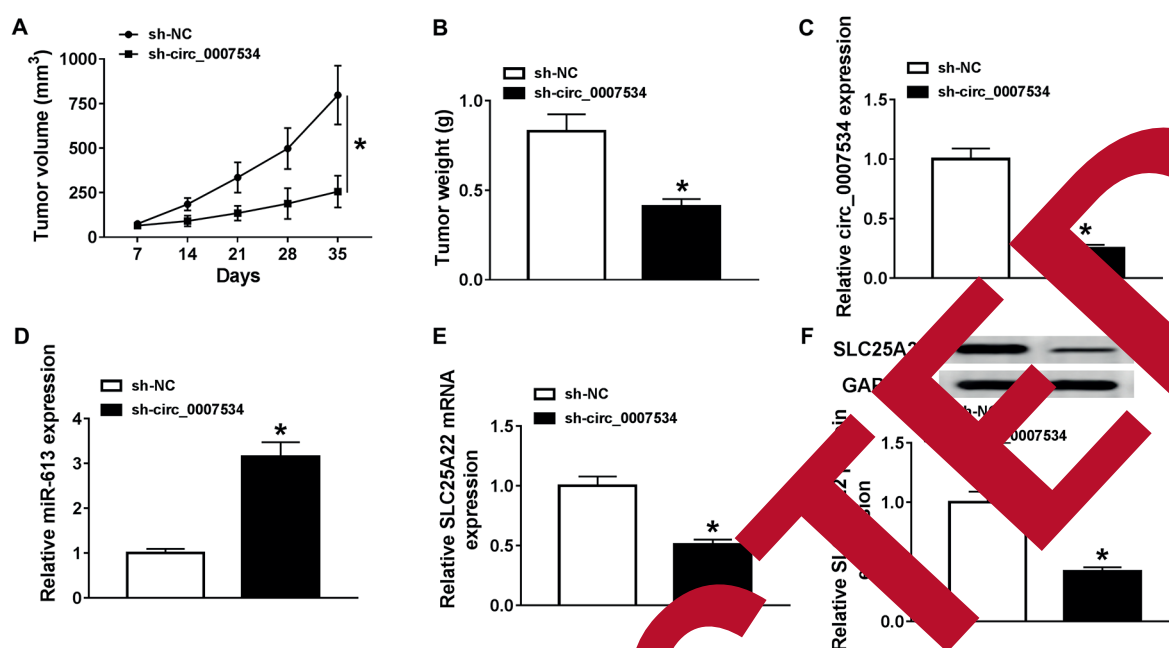


**Figure 8.** Circ\_0007534 knockdown attenuated tumor growth *in vivo*. **A**, Tumor volume was calculated in sh-circ\_0007534 group and sh-NC group every 7 d. **B**, Tumor weight was analyzed at 35 d of injection. **C**, The RNA levels of circ\_0007534, miR-613, and SLC25A22 were detected in sh-circ\_0007534 group and sh-NC group. **D**, The protein level of SLC25A22 was determined in sh-circ\_0007534 group and sh-NC group. \* $p < 0.05$ .

by repressing miR-613 expression. To confirm this hypothesis, LoVo and SW620 cells were transfected with si-NC, si-circ\_0007534, circ\_0007534 + anti-miR-NC, si-circ\_0007534 + anti-miR-613, respectively. Next, qPCR and Western blot assay revealed that SLC25A22 was downregulated by circ\_0007534 knockdown, and then partly rescued due to miR-613 depletion (Figure 7B). These results proved that circ\_0007534 repressed miR-613 expression to upregulate SLC25A22.

### Circ\_0007534 Depletion Repressed Tumor Growth *In Vivo*

To explore whether circ\_0007534 regulated tumor growth of CRC *in vivo*, the mice were subcutaneously injected with LoVo cells transfected with sh-circ\_0007534 or sh-NC. Then, we calculated tumor volume every 7 d, and found that the tumor was significantly smaller in sh-circ\_0007534 group than that in sh-NC group (Figure 8A). Moreover, tumor weight was downregulated by circ\_0007534 depletion (Figure 8B). Next, the levels of circ\_0007534, miR-613, and SLC25A22 were determined. As expected, the levels of circ\_0007534 and SLC25A22 were downregulated, and the level of miR-613 was

upregulated in sh-circ\_0007534 group (Figure 8C-F). Taken together, circ\_0007534 depletion repressed tumor growth *in vivo*.

## Discussion

Colorectal cancer is a common cancer with high metastasis rate worldwide<sup>24</sup>. Although some advanced technologies were used for its therapy, the treatment effect of most CRC patients still needs to be improved<sup>25</sup>. Thus, it is of importance to explore the mechanism of CRC development for the treatment of CRC patients. In this research, we investigated the functional mechanism of circ\_0007534 in CRC. The results demonstrated that circ\_0007534 knockdown suppressed the development of CRC by regulating miR-613/SLC25A22 axis.

Many circRNAs were reported to be involved in the development of CRC. Fang et al<sup>26</sup> confirmed that circ\_100290 knockdown repressed cell proliferation and mobility and promoted apoptosis *via* modulating miR-516b/ Frizzled-4 (FZD4) axis in CRC. Li et al<sup>27</sup> demonstrated that circ\_102958 promoted CRC development by regulation of miR-585/cell division cycle 25B (CDC25B) axis. Bian et al<sup>28</sup> showed that circ\_103809 negative-



ly regulated the growth of CRC cells by targeting miR-532-3p. In this research, we found that circ\_0007534 level was increased in CRC tissues and cells. Furthermore, circ\_0007534 knockdown suppressed the proliferation, colony formation, and mobility of CRC cells. Previous data indicated that circ\_0007534 acted as an oncogene in some cancers, including cervical cancer<sup>29</sup>, pancreatic ductal adenocarcinoma<sup>30</sup>, breast cancer<sup>31</sup>, glioma<sup>32</sup>, and CRC<sup>8</sup>. These findings agree with our results. Also, the effect of circ\_0007534 knockdown on glycolysis was explored in CRC cells. It is well known that glycolysis is enhanced in cancer cells<sup>33</sup>. It is a process in which glucose is converted into pyruvate accompanied by the production of lactate (fermentation). ECAR is an easily measurable indicator of glycolysis activity<sup>34</sup>. The inhibited ECAR, glucose consumption and lactate production revealed that glycolysis was suppressed. In addition, the levels of glycolysis-related proteins (such as HK2, GLUT1, and LDHA) can also be used to evaluate glycolysis. HK2 is the first rate-limiting enzyme in process of glycolysis<sup>35</sup>. GLUTs take charge of the transportation of glucose, and the overexpression of GLUTs facilitated glycolysis<sup>36</sup>. LDHA is an enzyme that converts pyruvate to lactate<sup>37</sup>. Thus, the down-regulated HK2, GLUT1, and LDHA resulted in the inhibition of glycolysis. Our results showed that circ\_0007534 knockdown indicated that circ\_0007534 knockdown repressed glycolysis in CRC cells.

CircDENND4C was highly expressed in breast cancer and promoted glycolysis<sup>38</sup>, meaning that circRNA, identified as an oncogene, might positively modulate glycolysis in human cancers. However, how circ\_0007534 affected glycolysis is unrevealed. Therefore, more experiments are needed to investigate the role of circ\_0007534 in CRC.

CircRNAs function as competing endogenous RNAs (ceRNAs) to regulate gene expression in cancer<sup>39</sup>. CircRNA-ACAP2 affected cell development by sponging miR-21-5p to regulate T lymphoma cell growth and metastasis protein 1 (Tiam1) in colon cancer<sup>40</sup>. To investigate the functional mechanism of circ\_0007534 in CRC, its target was explored. Using informatics tool starBase v2.0 and the Dual-Luciferase reporter assay, we found that circ\_0007534 targeted miR-613 and negatively regulated miR-613 expression. MiR-613 was reported to repress cell proliferation, migration, and invasion in a variety of cancers, including nasopharyngeal carcinoma<sup>41</sup>, colon cancer<sup>42</sup>, bladder cancer<sup>43</sup>, and retinoblastoma<sup>44</sup>. Moreover, Li et al<sup>14</sup> demonstrated that miR-613 was lowly expressed in CRC tissues/cells, and miR-613 sup-

pressed cell development. Also our results showed that miR-613 level was reduced in CRC tissues/cells compared with that in normal tissues/cells. In addition, miR-613 was shown to inhibit glycolysis metabolism in gastric cancer<sup>45</sup>. Taken together, it was speculated that circ\_0007534 regulated CRC cell progression *via* inhibiting miR-613 expression. Then, we sustained this hypothesis.

Zahid et al<sup>46</sup> showed that miRNAs exerted its function *via* targeting 3'-UTR of downstream mRNA. Here, through bioinformatics tool starBase v2.0 and the Dual-Luciferase reporter assay, we found that SLC25A22 was a target of miR-613, and SLC25A22 level was down-regulated by miR-613. SLC25A22 was a mitochondrial glutamate carrier<sup>47</sup>. In 2015, its function was analyzed in human cancers. Du et al<sup>48</sup> observed that SLC25A22 level was increased, and SLC25A22 promoted cell growth, as well as repressed apoptosis in gallbladder cancer. In CRC, SLC25A22 was highly expressed, and SLC25A22 accelerated cell proliferation. Our results demonstrated that SLC25A22 level was increased in CRC tissues and cells. The effect of SLC25A22 on glycolysis in human cancers was unknown. Wong et al<sup>20</sup> showed that the silence of SLC25A22 suppressed glycolysis in mice. These data suggested that SLC25A22 acted as a positive regulator in CRC development. Then, whether miR-613 regulates CRC by modulating SLC25A22 level was investigated in this study. As expected, miR-613 repressed the development of CRC cells *via* down-regulating SLC25A22 expression.

Finally, our results detected that circ\_0007534 inhibited miR-613 expression to upregulate SLC25A22 level in CRC cells, meaning that circ\_0007534 exerted its function by regulating miR-613/SLC25A22 axis. Next, the effect of circ\_0007534 on tumor growth was explored. As expected, circ\_0007534 depletion attenuated tumor growth *in vivo*.

## Conclusions

These findings demonstrated that circ\_0007534 knockdown suppressed the development of CRC by modulating miR-613/SLC25A22 axis, providing a theoretical basis for the therapy of CRC.

## Conflict of Interests

The Authors declare that they have no conflict of interests.

## References

- 1) BRENNER H, KLOOR M, POX CP. Colorectal cancer. *Lancet* 2014; 383: 1490-1502.
- 2) CHEN W, ZHENG R, BAADE PD, ZHANG S, ZENG H, BRAY F, JEMAL A, YU XQ, HE J. Cancer statistics in China, 2015. *CA Cancer J Clin* 2016; 66: 115-132.
- 3) BOPANNA S, ANANTHAKRISHNAN AN, KEDIA S, YAJNIK V, AHUJA V. Risk of colorectal cancer in Asian patients with ulcerative colitis: a systematic review and meta-analysis. *Lancet Gastroenterol Hepatol* 2017; 2: 269-276.
- 4) HSU MT, COCA-PRADOS M. Electron microscopic evidence for the circular form of RNA in the cytoplasm of eukaryotic cells. *Nature* 1979; 280: 339-340.
- 5) WANG Q, CHEN J, WANG A, SUN L, QIAN L, ZHOU X, LIU Y, TANG S, CHEN X, CHENG Y, CAO K, ZHOU J. Differentially expressed circRNAs in melanocytes and melanoma cells and their effect on cell proliferation and invasion. *Oncol Rep* 2018; 39: 1813-1824.
- 6) CHEN Q, LIU T, BAO Y, ZHAO T, WANG J, WANG H, WANG A, GAN X, WU Z, WANG L. CircRNA cRAP-GEF5 inhibits the growth and metastasis of renal cell carcinoma via the miR-27a-3p/TXNIP pathway. *Cancer Lett* 2020; 469: 68-77.
- 7) CHI G, XU D, ZHANG B, YANG F. Matrine induces apoptosis and autophagy of glioma cell line U951 by regulation of circRNA-104075/BCL-9. *Cell Mol Biol Interact* 2019; 308: 198-205.
- 8) ZHANG R, XU J, ZHAO J, WANG X. Silencing of circ\_0007534 suppresses proliferation and induces apoptosis in colorectal cancer cells. *Eur J Med Pharmacol Sci* 2018; 22: 1-10.
- 9) YANG Q, PAN W, QIAN L. Identification of the miR-NA-mRNA regulatory network in multiple sclerosis. *Neurol Res* 2017; 39: 142-151.
- 10) TUTAR Y. MiRNA applications and experimental approaches. *Current Form Biotechnol* 2014; 15: 429.
- 11) QADIR MI, FAROOQ MI. MicroRNA: a diagnostic and therapeutic tool for pancreatic cancer. *Crit Rev Eukaryot Gene Expr* 2015; 25: 197-204.
- 12) WANG H, HU K, CHAO Y, WANG X. MicroRNA-1296-5p suppresses the proliferation, migration, and invasion of human osteosarcoma cells by targeting CH22. *Cell Biochem* 2020; 121: 2038-2046.
- 13) ZHANG L, ZHANG L, WANG B, WEI R, WANG Y, WAN J, ZHANG L, CHAO L, LIU X, ZHANG Y, CHU C, GUO Q, LIU X, LIU B. miR-613-3p suppresses proliferation of epithelial colorectal cancer by targeting PIK3CA and PIK3CB. *Cancer Lett* 2020; 469: 54-67.
- 14) ZHANG L, ZHANG L, WANG B, WEI R, WANG Y, WAN J, ZHANG L, CHAO L, LIU X, ZHANG Y, CHU C, GUO Q, LIU X, LIU B. miR-613-3p suppresses proliferation of epithelial colorectal cancer by targeting PIK3CA and PIK3CB. *Cancer Lett* 2020; 469: 54-67.
- 15) ZHANG L, ZHANG L, WANG B, WEI R, WANG Y, WAN J, ZHANG L, CHAO L, LIU X, ZHANG Y, CHU C, GUO Q, LIU X, LIU B. miR-613-3p suppresses proliferation of epithelial colorectal cancer by targeting PIK3CA and PIK3CB. *Cancer Lett* 2020; 469: 54-67.
- 16) GOUBERT E, MIRCHEVA Y, LASORSA FM, MELON C, PROFILO E, SUTERA J, BECO H, PALMIERI F, PALMIERI L, ANIKSZTEJN L, MOLINARI F. Inhibition of the mitochondrial glutamate carrier SLC25A22 in astrocytes leads to intracellular glutamate accumulation. *Front Cell Neurosci* 2017; 11: 149.
- 17) DU P, LIANG H, FU X, WU P, WANG C, CHEN J, ZHENG B, ZHANG J, HU S, ZENG R, LIANG B, FANG G. SLC25A22 promotes proliferation and metastasis by activating MAPK/ERK pathway in gallbladder cancer. *Cancer Cell Int* 2019; 19: 30.
- 18) CHEN MW, WU XJ. SLC25A22 promotes proliferation and metastasis of osteosarcoma cells via the PTEN signaling pathway. *Tumor Cancer Treat* 2018; 17: 1533-1538.
- 19) LI X, CHUNG H, LI S, CHEN X, XU J, YU J, WONG C, CAI Z. LCMS-based metabolomics revealed SLC25A22 as an essential transporter of aspartate-derived amino acids and polyamines in KRAS-mutant colorectal cancer. *Oncotarget* 2017; 8: 101333-101343.
- 20) CHEN Q, QIAN Y, LI X, WANG W, TONG JH, TO KF, JIN Y, LI W, CHEN H, GO MW, WU JL, CHENG KW, NG SS, SUNG JJ, CAI Z, YU J. SLC25A22 promotes proliferation and survival of colorectal cancer cells with KRAS mutation and xenograft tumor progression in mice via intracellular synthesis of aspartate. *Cancer Cell Int* 2016; 151: 945-960.e6.
- 21) CHEN L, QIU J, YANG C, YANG X, CHEN X, JIANG J, LUO Y. Identification of a novel estrogen receptor binding partner, inhibitor of differentiation-1, and role of ERbeta1 in human breast cancer cells. *Cancer Lett* 2009; 278: 210-219.
- 22) FLAVENY CA, GRIFFETT K, EL-GENDY BEL D, KAZANTZIS M, SENGUPTA M, AMELIO AL, CHATTERJEE A, WALKER J, SOLT LA, KAMENECKA TM, BURRIS TP. Broad anti-tumor activity of a small molecule that selectively targets the warburg effect and lipogenesis. *Cancer Cell* 2015; 28: 42-56.
- 23) KAWAUCHI K, ARAKI K, TOBIUME K, TANAKA N. p53 regulates glucose metabolism through an IKK-NF-kappaB pathway and inhibits cell transformation. *Nat Cell Biol* 2008; 10: 611-618.
- 24) BRODY H. Colorectal cancer. *Nature* 2015; 521: S1.
- 25) HARRIS TJ, McCORMICK F. The molecular pathology of cancer. *Nat Rev Clin Oncol* 2010; 7: 251-265.
- 26) FANG G, YE BL, HU BR, RUAN XJ, SHI YX. CircRNA\_100290 promotes colorectal cancer progression through miR-516b-induced downregulation of FZD4 expression and Wnt/beta-catenin signaling. *Biochem Biophys Res Commun* 2018; 504: 184-189.
- 27) LI R, WU B, XIA J, YE L, YANG X. Circular RNA hsa\_circRNA\_102958 promotes tumorigenesis of colorectal cancer via miR-585/CDC25B axis. *Cancer Manag Res* 2019; 11: 6887-6893.
- 28) BIAN L, ZHI X, MA L, ZHANG J, CHEN P, SUN S, LI J, SUN Y, QIN J. Hsa\_circRNA\_103809 regulated the cell proliferation and migration in colorectal cancer via miR-532-3p / FOXO4 axis. *Biochem Biophys Res Commun* 2018; 505: 346-352.

- 29) RONG X, GAO W, YANG X, GUO J. Downregulation of hsa\_circ\_0007534 restricts the proliferation and invasion of cervical cancer through regulating miR-498/BMI-1 signaling. *Life Sci* 2019; 235: 116785.
- 30) HAO L, RONG W, BAI L, CUI H, ZHANG S, LI Y, CHEN D, MENG X. Upregulated circular RNA circ\_0007534 indicates an unfavorable prognosis in pancreatic ductal adenocarcinoma and regulates cell proliferation, apoptosis, and invasion by sponging miR-625 and miR-892b. *J Cell Biochem* 2019; 120: 3780-3789.
- 31) SONG L, XIAO Y. Downregulation of hsa\_circ\_0007534 suppresses breast cancer cell proliferation and invasion by targeting miR-593/MUC19 signal pathway. *Biochem Biophys Res Commun* 2018; 503: 2603-2610.
- 32) LI GF, LI L, YAO ZQ, ZHUANG SJ. Hsa\_circ\_0007534/miR-761/ZIC5 regulatory loop modulates the proliferation and migration of glioma cells. *Biochem Biophys Res Commun* 2018; 499: 765-771.
- 33) ZHANG Y, YANG JM. Altered energy metabolism in cancer: a unique opportunity for therapeutic intervention. *Cancer Biol Ther* 2013; 14: 81-89.
- 34) KALYANARAMAN B, CHENG G, HARDY M, OUARI O, LOPEZ M, JOSEPH J, ZIELONKA J, DWINELL MB. A review of the basics of mitochondrial bioenergetics, metabolism, and related signaling pathways in cancer cells: therapeutic targeting of tumor mitochondria with lipophilic cationic compounds. *Redox Biol* 2018; 14: 316-327.
- 35) LINCET H, ICARD P. How do glycolytic enzymes affect your cancer cell proliferation by nonmetabolic functions? *Oncogene* 2015; 34: 3750-3759.
- 36) MACHEDA ML, ROGERS S, BESTERMAN J. Molecular and cellular regulation of glucose transporters (GLUT) proteins in cancer. *J Cell Physiol* 2005; 203: 654-662.
- 37) GANAPATHY-KANNIAPPAN S, CHANDRANIDHI S. Autophagy as a target for cancer therapy: progress and prospects. *Cancer* 2014; 125: 149-152.
- 38) REN S, LIU J, LIU Z, HE L, LI Y, LIU X, WANG Z, ZHANG Y. Knockdown of circDENND4C inhibits glycolysis, migration and invasion by up-regulating miR-200b/c in breast cancer under hypoxia. *J Exp Clin Cancer Res* 2019; 38: 388.
- 39) XIONG DD, DANG YW, LIN P, WEN DY, HE RQ, LUO DZ, FENG ZB, CHEN G. A circRNA-miRNA-mRNA network identification for exploring underlying pathogenesis and therapy strategy of hepatocellular carcinoma. *J Transl Med* 2018; 16: 220.
- 40) HE JH, LI YG, HAN ZP, ZHOU JB, CHEN Y, LIU Y, HE ML, ZUO JD, ZHENG L. The CircRNA-ACAP2-Hsa-miR-21-5p/Tiam1 regulatory feedback circuit affects the proliferation, migration and invasion of colon cancer SW480 cells. *Cell Physiol Biochem* 2018; 49: 1539-1550.
- 41) GAO R, FENG Q, TAN G. MicroRNA-613 exerts an anti-angiogenic effect on nasopharyngeal carcinoma cells through inhibiting the AKT signaling pathway by down-regulating VEGF1. *Biosci Rep* 2019; 39: pii: 180218.
- 42) DONG Y, WANG H, LU JG, LIU J. Long non-coding RNA HULNC1 interacts with miR-613 to regulate colon cancer growth and metastasis through targeting VTKN. *Drug Discov Pharmacother* 2019; 109: 2035-2042.
- 43) LIU J, LIU P, ZHU H, LIU Y, LIU X, LIU Y, LIU X, LIU P, ZHU H, LIU Y, LIU X. MiR-613 inhibits bladder cancer proliferation and migration through targeting SphK1. *Am J Transl Res* 2017; 9: 1213-1221.
- 44) ZHANG Y, ZHANG Y, ZHU X, WU Y, LIU Y, YAO B, LIU Z. MiR-613 suppresses retinoblastoma cell proliferation, invasion, and tumor formation by targeting E2F5. *Tumour Biol* 2017; 39: 1010428317691674.
- 45) LIU J, LIU P, CHEN K, WANG L, ZENG X, HUANG Z, LI M, LIU P, CHEN X. MiR-613 inhibits Warburg effect in gastric cancer by targeting PFKFB2. *Biochem Biophys Res Commun* 2019; 515: 37-43.
- 46) ZAHID KR, SU M, KHAN ARR, HAN S, DEMING G, RAZA U. Systems biology based meth-miRNA-mRNA regulatory network identifies metabolic imbalance and hyperactive cell cycle signaling involved in hepatocellular carcinoma onset and progression. *Cancer Cell Int* 2019; 19: 89.
- 47) CASIMIR M, LASORSA FM, RUBI B, CAILLE D, PALMIERI F, MEDA P, MAECHLER P. Mitochondrial glutamate carrier GC1 as a newly identified player in the control of glucose-stimulated insulin secretion. *J Biol Chem* 2009; 284: 25004-25014.